Oxygen reduction reaction catalyzed by cobalt(III) complexes of macrocyclic ligands supported on multiwalled carbon nanotubes

ARTICLE *in* CHEMICAL PHYSICS LETTERS · APRIL 2013

Impact Factor: 1.9 · DOI: 10.1016/j.cplett.2013.02.046

6 AUTHORS, INCLUDING:

Udaya B. Nasini
U.S. Food and Drug Administration
17 PUBLICATIONS **96** CITATIONS
SEE PROFILE

Yashraj Gartia
Bayer Health Care, Kansas
18 PUBLICATIONS **121** CITATIONS
SEE PROFILE

Chemical Physics Letters 566 (2013) 38–43

Contents lists available at SciVerse ScienceDirect

Chemical Physics Letters

journal homepage: www.elsevier.com/locate/cplett

Oxygen reduction reaction catalyzed by cobalt(III) complexes of macrocyclic ligands supported on multiwalled carbon nanotubes

Udaya B. Nasini [a], Yashraj Gartia [a], Punnamchandar Ramidi [a], Abul Kazi [b], Ali U. Shaikh [a,*], Anindya Ghosh [a,*]

[a] Department of Chemistry, University of Arkansas at Little Rock, Little Rock, AR 72204, United States
[b] Department of Chemistry and Physics, University of Arkansas at Pine Bluff, Pine Bluff, AR 71601, United States

ARTICLE INFO

Article history:
Received 17 January 2013
In final form 19 February 2013
Available online 26 February 2013

ABSTRACT

A class of amido-macrocyclic cobalt(III) complexes along with multiwalled carbon nanotubes have been studied for electro-catalytic activity to reduce oxygen. These complexes are efficient for oxygen reduction reaction (ORR) in wide range of pH conditions by following ideal fuel cell reduction mechanism. Depending on the stability of complexes in different pH, electrochemical studies were performed to predict the reduction mechanism. Rotating disk electrode and rotating ring-disk electrode studies show that these complexes reduce oxygen via four electron reduction process in mild acidic pH and two step two electron reduction processes in basic conditions, with negligible amount of hydrogen peroxide generation.

1. Introduction

We heavily depend on fossil fuels (coal, natural gas and oil) to meet our energy needs. One major problem with burning fossil fuels is the generation of a large quantity of CO_2 that is linked to global warming [1]. Another problem concerns the low efficiency (<30%) of the fossil fuel powered sources as they are thermodynamically limited both in the Rankin and Carnot engines [2]. There is, therefore, a critical need for a clean, economic energy production technology that will meet our growing needs. The use of hydrogen as fuel in fuel cells is considered one of the most promising possibilities for an energy solution [3–8]. Hydrogen can be combined with oxygen in a fuel cell to produce energy by electrochemical reaction [9,10]. The process is environmentally clean, the reaction product is only water, and considered a carbon–neutral process as hydrogen can be produced from renewable resources, such as wind, solar, thermal electrolysis, etc. [11]. In addition to the above-mentioned advantages, electrochemical energy generation devices such as fuel cells can theoretically be much more efficient compared to conventional ways of producing energy using fossil fuels [12,13].

Commercially available hydrogen–oxygen fuel cells utilize platinum as the catalyst for both cathode and anode reactions in acidic and alkaline media, according to the reactions below:

$$\text{A. In acidic medium}: O_2 + 4H^+ + 4e^- \rightarrow 2H_2O \text{ at the cathode}$$
$$H_2 \rightarrow 2H^+ + 2e^- \text{at the anode}$$
$$\text{In alkaline medium}: O_2 + 2H_2O + 4e^- \rightarrow 4OH^- \text{at the cathode}$$
$$H_2 \rightarrow 2H^+ + 2e^- \text{at the anode}$$

The cathode reaction on a platinum electrocatalyst (either platinum metal or particulate mixed with carbon) in acidic medium is unequivocally established to be a direct four proton/four electron reduction of oxygen to water. In an alkaline medium, however, the reaction is believed to proceed in two steps, producing peroxide as an intermediate [14].

$$\text{Step 1}: O_2 + H_2O + 2e^- \rightarrow HO_2^- + OH^-;$$
$$\text{Step 2}: HO_2^- + H_2O + 2e^- \rightarrow 3OH^-$$

The production of peroxide is undesirable as it causes deactivation of the electrode. Moreover, a direct four electron reduction produces higher voltage than two consecutive two electron reductions. The primary drawbacks of platinum as catalyst, particularly for the cathode reaction, is its high time-dependent drift in voltage, methanol crossover, and carbon monoxide deactivation [14]. Most importantly platinum is highly scarce on earths's crust and a very expensive metal. This is one of the major reasons for the high cost of producing electricity using hydrogen–oxygen fuel cells, and thus commercialization of the technology is very difficult. Nevertheless, platinum is the best choice at this time for fuel cells at it provides the highest voltage at rapid and sustained rate, compared to any other (non-platinum) catalyst that have been developed.

Extensive efforts are being made to develop new catalysts for replacing expensive Pt-catalysts for the oxygen reduction reaction (ORR) at the cathode [15]. Most of these studies involve nano

* Corresponding authors. Fax: +1 501 569 8838 (A. Ghosh), Fax: +1 501 569 8838 (Ali U. Shaikh).
E-mail addresses: aushaikh@ualr.edu (A.U. Shaikh), axghosh@ualr.edu (A. Ghosh).

0009-2614/$ - see front matter © 2013 Elsevier B.V. All rights reserved.
http://dx.doi.org/10.1016/j.cplett.2013.02.046

particulate forms of platinum mixed with carbon (to reduce Pt loading in order to minimize cost) and other noble bulk metals such as Au, Ag, Pd, Ru and Cu, as well as their alloys and oxides [16,17]. In 1964, Jasinski reported [18] for the first time that transition metal porphyrins and phthalocyanines show electrocatalytic activity toward ORR. Most of these complexes, particularly cobalt and iron porphyrins, showed ORR in two consecutive two-electron reduction processes involving hydrogen peroxide as the intermediate:

$$O_2 + 2H^+ + 2e^- \rightarrow H_2O_2; \quad H_2O_2 + 2H^+ + 2e^- \rightarrow 2H_2O$$

The result is significant reduction in voltage output for such fuel cells. The electrocatalyst is deactivated by hydrogen peroxide as well. Further research showed that several cobalt and iron porphyrins, pthalocyanins, corroles and salens were capable of direct four electron reduction of oxygen to water in acidic media [19–25]. Most of these complexes are N_4 macrocycles with MN_4 (M = Co, Fe) centers where ORR activity occurs. These complexes, however, are unstable at very low pH (<1.0) and, therefore, not suitable as electrocatalysts for polymer electrolyte membrane fuel cells (PEMFCs). Moreover, the mechanism of ORR varies in acidic and alkaline media, with less than four electron direct reduction of oxygen to water. However, they could be suitable for ORR activity in microbial fuel cells (MFCs) and enzymatic biofuel cells (EBCs), where ORR activity can be utilized in neutral, weakly acidic or weakly basic environments to produce electricity [26–29].

In, this report we describe a series of cobalt(III) amido-macrocyclic (MN_4) complexes, having two N-atoms attached to an aromatic ring carrying various substituents, which show direct four electrons ORR process in reaction media of wide pH range from 0.0 to 9.0. Similar iron (III) amido macrocyclic complexes exhibit excellent reactivity towards both oxygen [30] and hydrogen peroxide [31] in neutral media. Few similar cobalt(III) complexes are known in the literature but other than activation of epoxides for catalytic cyclic carbonate synthesis no such electrocatalytic reactivity has been studied [32]. Based on the literature studies [33–36] the effect of MWCNTs on the ORR activity of these complexes has been studied.

2. Experimental

All reagents were of analytical grade and used without further purification unless stated otherwise. Most of the chemicals and solvents used to synthesize the metal complexes and electrochemical characterizations were obtained either from Aldrich Chemical Company, USA or Fisher Scientific Company, USA. Multiwalled carbon nanotubes (MWCNTs) were purchased from Bayer Group (BaytubesC 150P, 95% purity) and used as received. Ultra-violet visible (UV/Vis) spectra were recorded using a Varian Carey V spectrophotometer. Electrospray ionization mass spectrometry (ESI-MS) was performed using an Agilent Model 1100 LC-Ion-Trap. Scanning electron microscopy (SEM) and EDX (Energy-dispersive X-ray spectroscopy) analysis was carried by using JEOL SEM (JSM 7000F). Elemental analysis was performed in the Midwest Micro Lab, LLC (Indianapolis, IN).

2.1. Synthesis of ligands and metal complexes

Synthesis of the cobalt amido complexes (Figure 1) has been performed by inserting Co(II) into the amido ligand by deprotonation using *n*-butyl lithium, followed by the addition of cobalt(II)chloride. Stirring the mixture overnight produced an insoluble cobalt amido-complex. Different amido complexes were synthesized by changing the pendant groups on the aromatic ring [32]. SEM characterization of the 1c complex mixed with MWCNTs and nafion® showed the homogeneous coating of nafion® on the surface of MWCNTs preserving the tubular structures of pristine MWCNTs (Figure S1, supporting information). EDX analysis of 1c on MWCNTs showed 1.15% (wt.%) of cobalt in the active surface area, presented in Table S1, supporting information.

2.2. Electrochemical studies

Electrochemical experiments (cyclic voltammetry and rotating ring-disk voltammetry) were conducted using a Pine Instruments (Raleigh, NC) bipotentiostat having three and four electrode probe systems. A 0.50 M H_2SO_4 solution (calc. pH = 0.0) was prepared by diluting concentrated sulfuric acid. Solutions of pH 4.0, 7.0 and 9.0 were prepared using wide range buffer mixtures composed of boric acid (anhydrous), citric acid (monohydrate) and tertiary sodium phosphate (decahydrate) using published procedure [37]. All buffer solutions and dilutions were made using deionized water. The experiments were conducted in oxygen-saturated solutions to measure oxygen reduction reaction. To check the electrochemical activity of the complexes, solutions were purged with high purity nitrogen (Airgas) to remove oxygen. Cyclic voltammetry were conducted using glassy carbon disks (Bioanalytical Systems, Lafayette, IN) as the working electrode. For RRDE studies, the graphite disk-platinum ring electrode and MSR speed control rotor were purchased from the Pine instruments (Raleigh, NC). The reference electrodes were Ag/AgCl and Hg/HgO electrodes (Pine Instruments) for acidic and alkaline media as appropriate, and the counter electrode was a platinum wire (Bioanalytical Systems). All experiments were conducted at room temperature (22 °C). The electrochemical cell was a 100 mL glass container with a three holed rubber cap through which electrodes were inserted.

2.2.1. Deposition of electrocatalyst on the electrode

A homogeneous 1 mg/mL solution of cobalt composite was prepared by dissolving 5.0 mg of the catalyst in 5.0 mL of THF. A 2:1 ratio mixture of catalyst to MWCNTs prepared and sonicated for 30 min to get a homogeneous dispersion. To 0.5 mL of this solution 20 μL of nafion® (5 wt.%) was added, which acts as a medium for proton transport [38]. The resulting homogenous mixture was ultrasonicated for about 30 min. For cyclic voltammetry, a 10 μL aliquot of the mixture was placed on the glassy carbon electrode (the working electrode) and dried under high vacuum to get a uniform thin layer. For RRDE studies, a similar procedure was followed to deposit the composite solution on the disk portion of the ring-disk electrode and avoiding the platinum ring completely. RRDE polarization curves were recorded with various rotations speeds (100, 400, 900, 1600, 2500 and 3600 rpm). Oxygen reduction was

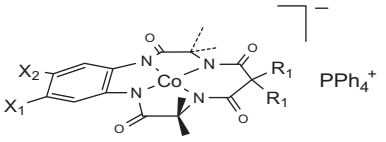

Catalyst	X_1	X_2	R_1
1a	H	H	CH_3
1b	H	COOH	CH_3
1c	H	NO_2	CH_3

Figure 1. Different Cobalt(III)-amido macrocyclic metal complexes used in this study for oxygen reduction.

recorded on the disk electrode at the potential range determined by cyclic voltammetry of the complexes. The potential of the ring electrode was held at 0.60 V, 0.80 V and 1.0 V to monitor any generation of H_2O_2. Multiple layers of the electrocatalysts were deposited on the same electrode surface in the same way as described above for further studies.

3. Results and discussion

The compounds studied here contain a cobalt (MN_4) center, where oxygen is supposed to undergo reduction, and a pendant group of varying electron withdrawing capability. The pendant groups are –H (Compound 1a), –COOH (Compound 1b) and $–NO_2$ (Compound 1c), having different electron withdrawing capability. These compounds are highly soluble in water when the cation is Li^+ but become insoluble when the cation is PPh_4^+ (Figure 1). In order to perform ORR electrochemistry in aqueous solution, therefore, the insoluble form was drop-casted on a glassy carbon or platinum electrode. A uniform thin layer of the complex can easily be created, either by single or multiple drop casting.

Cyclic voltammograms of the three complexes (1a–1c) at pH 4.0 are shown in Figure 2. Excellent oxygen reduction peaks are shown by all three complexes, with oxygen reduction peak potentials at −0.31 V, −0.28 V and −0.24 V (vs. Ag/AgCl), respectively. Obviously, the pendant group has a profound effect on the ORR capability of the compounds. As the electron-withdrawing effect of the pendant group increases, so also the ease of reduction of oxygen. Similar effects were observed in Co(II) MN_4 complexes with porphyrins [24,39,40]. It is, therefore, likely that strongly electron-withdrawing pendant groups (such as –F) at a single or multiple positions will reduce the ORR overvoltage greatly, thus increasing the voltage output.

Since the $–NO_2$ subtituted MN_4 complex (Compound 1c) has the most positive ORR potential, detailed electrochemical studies are presented with this compound, although all three compounds behave very similarly. When mixed with nanotubes, a redox potential shift of about +40 mV was observed for the oxygen reduction (Figure 3). Similar shift with other MN_4 electrocatalyst in the presence of nanotubes have been reported [41] although some porphyrins (hangman porphyrins, for example) do not show a similar shift [24]. The enhanced catalytic activity of the complex mixed with MWCNTs could be due to stabilization of the complex by π–π stacking on nanotubes and the participation of nanotubes in the electron transfer process [25]. The synergistic effect of MWCNTs was evaluated by changing the ratio of MWCNTs to complex 1c concentration. We doubled the proportion of MWCNTs with respect to the concentration of complex 1c (2:1); ORR current density increased two folds, compared to MWCNTs to complex 1c ratio 1:1 as shown in the Figure 4. An increase in the concentration of complex 1c with decreased MWCNTs composition did not show better ORR current density when compared with 2:1 ratio of MWCNTs and complex 1c. The ORR stability of the complex increases significantly when mixed with MWCNT. In the pH range of 4.0 to 10.0, MWCNT/Co(III) composite showed no loss in ORR current density for repeated use over a period of over six months. At pH lower than 4.0 and higher than 10.0, the composite loses stability in about a month of repeated use.

Figure S2 (supporting information) shows the visible spectrum of the soluble form of the compound in various pH media. It is evident that the compound is not very stable at extreme pH values, although some stability is observed at pH 0.0. However, the compound is highly stable in the pH range of 4.0–9.0. No apparent loss in the absorption peak was observed over a period of several months.

Cyclic voltammetric studies of the insoluble form (when drop-casted on a glassy carbon electrode) showed that the ORR peak potential and current density remained stable for over two months in buffer solutions of pH 2.0–10.0, although rapid loss occurred at pH 0.0 after about half an hour due to demetallation. At pH 14.0, the

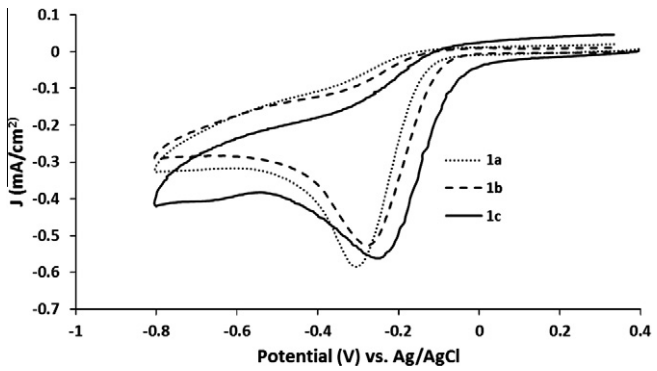

Figure 2. Cyclic voltammetry of 1a–1c (without MWCNTs) deposited on glassy carbon electrode in oxygen saturated pH 4.0 buffer solution, scan rate 100 mV/s, reference to the Ag/AgCl electrode. Anodic peak of each complex is different due to structural differences.

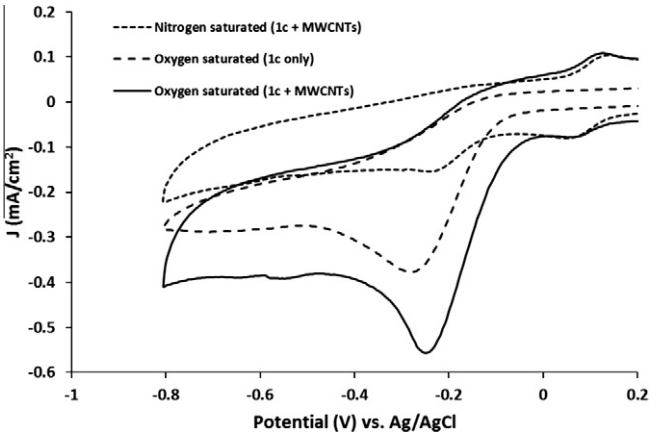

Figure 3. Comparison of cyclic voltammograms of MWCNTs supported electrocatalyst 1c (1:1 ratio) and electrocatalysts itself in nitrogen and oxygen saturated pH 4.0 buffer.

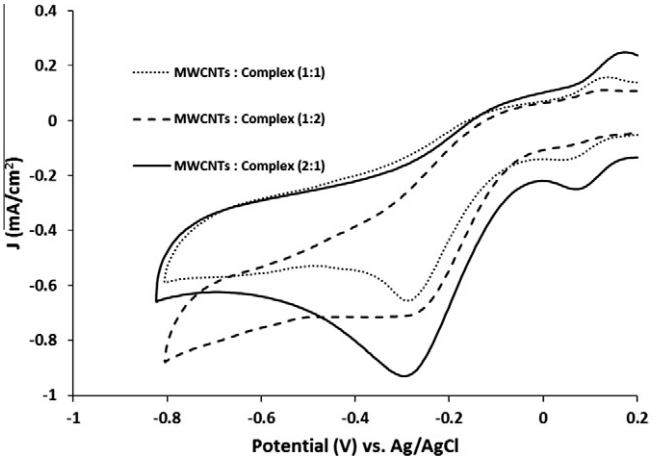

Figure 4. Cyclic voltammograms of MWCNTs-Complex using different ratios of nanotubes to complex concentration.

dropcasted layer of the compound dissolved very rapidly, probably due to hydrolysis of the amido complex forming cobalt hydroxide.

Figure S3 (supporting information) shows the effect of dropcasting of multiple layers of the MWCNTs supported electrocatalyst on ORR activity. The current density almost three times after six layers are drop casted; this is obviously due to an increase in the number of active cobalt centers per unit geometrical surface area of the electrode. No significant current enhancement was observed beyond six layers. Similar behavior has been reported with cobalt porphyrin electrocatalysts [11,23]. CV of MN_4 complexes in nitrogen purged pH 4.0 buffer media demonstrates that the reduction potential for Co(III/IV) in the range of −0.60 V to 0.0 V (Figure 3), indicating the reduction peak of reversible anodic for one electron oxidation of Co(III)–Co(IV).

Figure 5 shows the effect of pH on the ORR potential. As the pH is increased from 0.0 to 14.0, the peak potential shifts to more negative values, as expected, while the current density remains fairly constant. This indicates that the electrocatalyst efficiency is not minimized as the pH is increased (with less H^+ available), although the reaction mechanism may be changing from four proton/four electron reduction (at low pH) to reduction involving water molecules (See *Introduction*). A plot of the ORR peak potential vs. pH reveals that the two linear segments of the graph intersect at around pH 6.0 (Figure S4, see supporting information). It is postulated, therefore, that the mechanism of oxygen reduction is predominantly H^+ based below pH 6.0 and is H_2O based above pH 6.0. The calculated slope of the line (below pH 6.0) is −0.059 volt, which indicates that the ORR process involves four protons and 4 electrons: $O_2 + 4H^+ + 4e^- \rightarrow 2H_2O$. Also, if the ORR is a single four electron electrochemically reversible process, the theoretical shift in peak potential should be −0.354 volt at 22 °C as the pH is changed from 0.0 to 6.0 [38]. The observed shift is ca. −0.400 volt, slightly higher than that for the reversible process. This indicates that the process involves some electrochemical irreversibility (due to kinetic effect) even though it may be a single step four electron process. The magnitude of the slope above pH 6.0 is less than 0.059 volt, which indicates that the ORR mechanism has been promoted by not a single four electron process, but multiple processes as follows [14]:

$$\text{Step 1}: O_2 + H_2O + 2e^- \rightarrow HO_2^- + OH^-;$$
$$\text{Step 2}: HO_2^- + H_2O + 2e^- \rightarrow 3OH^-$$

Further evidence in support of this observation is presented below.

In order to assess the catalytic activity of these complexes at various pH we performed rotating disk electrode (RDE) and rotating ring disk electrode (RRDE) experiments. Figure 6a shows RDE curves for compound 1c at pH 4.0. Similar studies at other pH values are given in the Supplementary Section (Figure S5, supporting information).

To find the number of electrons involved in the oxygen reduction mechanism, limiting currents were obtained from the RDE plots (Figure 6). Koutecky–Levich equation can be used to calculate the Levich current (J_{lev}) and the kinetic current (J_k), according to the equation

$$1/j_{\text{lim}} = 1/j_{Lev} + 1/J_k$$

where, $J_{Lev} = 0.620nFCD^{2/3}\omega^{1/2}\upsilon^{-1/6}$ (n = number of electrons transferred in the half reaction, F = Faraday constant = 96486.4 Coulombs, C = molar concentration of analyte (oxygen) = 2.4×10^{-4} M at 25 °C, D = diffusion coefficient of oxygen in water at 25 °C = 1.7×10^{-5} cm^2/s, υ = kinematic viscosity of the solution at 25 °C = 0.01 cm^2/s, and ω = angular rotation rate of the electrode = $2\pi N$ (N = linear rotation speed); j_k = rate of kinetically limited reaction = $10^3nFkC\Gamma$ (k = rate constant for the oxygen reduction, Γ = concentration of catalyst on electrode mol/cm^2).

By plotting the graph between $1/j_{\text{lim}}$ and $\omega^{-1/2}$ gives the slope of $1/0.620nFCD^{2/3}\upsilon^{-1/6}$. Resulting experimental plots using Koutecky–Levich equation and the theoretical plots (assuming $n = 2$ and $n = 4$) were compared to check the number of electrons involved in the oxygen reduction. Figure 7 shows the Koutecky–Levich plot of oxygen reduction at pH 4.0. Similar plots at higher pH values are given in Figure S6 of supporting information. Overall, the rate constant remains in the range of 10^5, which is quite high and comparable to other Cobalt MN_4 electrocatalysts [22,23].

Number of electrons (n) participated in the ORR are also calculated by RRDE information (Fig 6b) using the following equation.

$$n = 4I_{\text{disk}}/(I_{\text{disk}} + I_{\text{ring}}/N)$$

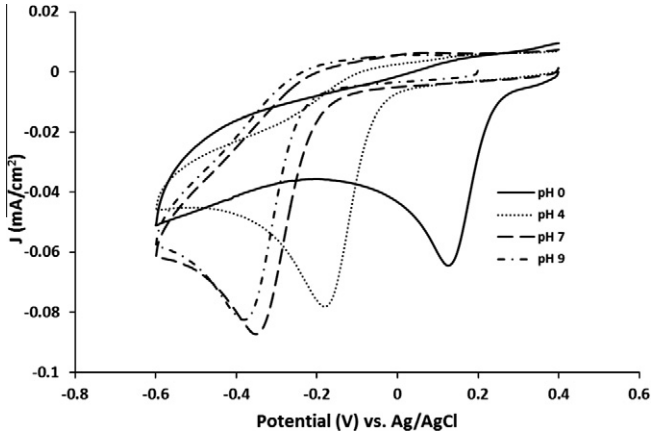

Figure 5. Cyclic voltammograms of complex 1c (mixed with nafion®) in oxygen saturated solutions of different pH at 25 °C.

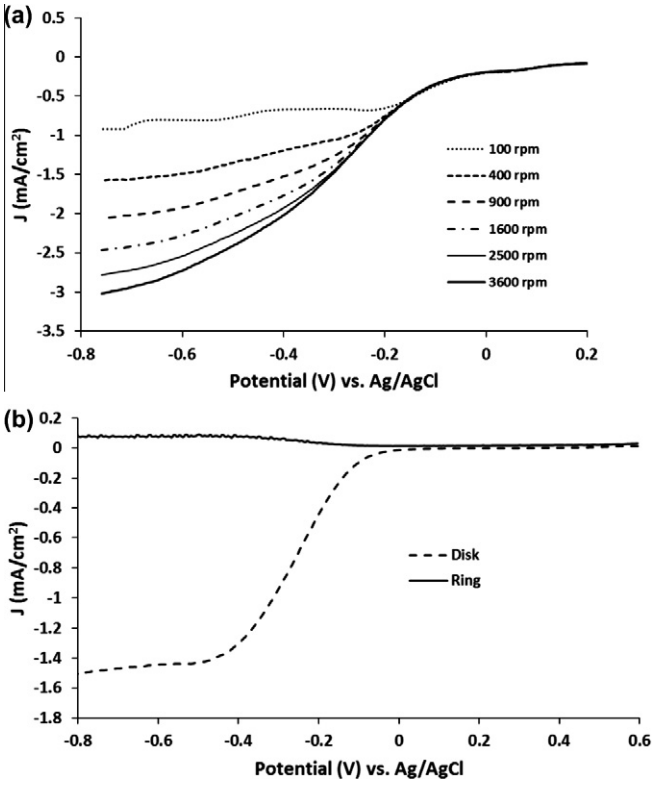

Figure 6. (a) RDE curves for the reduction of oxygen at 25 °C at a) pH 4.0 in oxygen saturated buffer solution, (b) RRDE curves at 2500 rpm holding ring potential at 1.0 V.

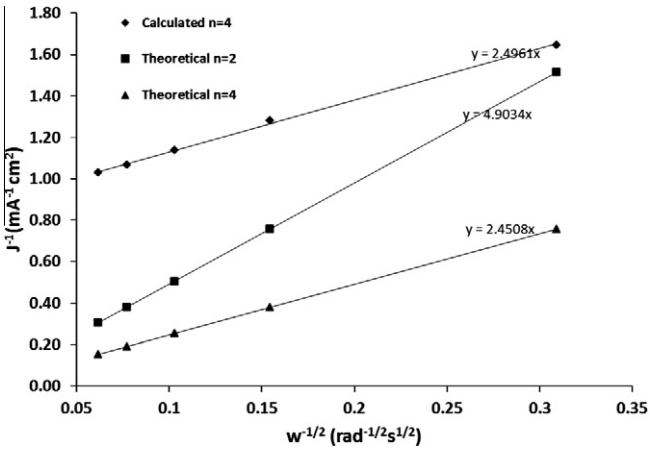

Figure 7. Koutecky–Levich plot of RDE of oxygen reduction at pH 4.0.

Table 1
Number of electrons calculated from RDE and RRDE data and rate constants in oxygen saturated buffer solution at different pH conditions.

pH	*n* (Koutecky–Levich Plot)	*n* (RRDE data at 2500 rpm)	J_k (Koutecky–Levich Plot)	*k* ($mol^{-1}\ s^{-1}$)
2.0	3.95	3.92	0.639	1.62×10^5
4.0	3.74	3.99	0.958	1.14×10^5
7.0	4.31	3.90	0.830	1.14×10^5
9.0	4.14	4.00	0.635	1.55×10^5

Table 1 shows the calculated values of *n*, J_k, and *k* for ORR at different pH solutions in oxygen saturated electrolytes. At low concentrations of catalyst ($\Gamma = 1.06 \times 10^{-10}$ mol cm^{-2}) the rate constant for oxygen reduction increases with an increase in the pH of the medium. However, then it remains in the range of 10^5 for the entire pH range (2.0–9.0) which is quite high and comparable to other Cobalt MN_4 electrocatalysts [23]. The catalyst, therefore, has an excellent capability of reducing oxygen by four electron mechanism. In the presence of protons (acidic media) the reduction takes place by direct conversion of oxygen to water with negligible amount of hydrogen peroxide generation. In alkaline condition, it appears to follow also a one-step four electron process, as demonstrated by RDE results at pH 7.0 and pH 9.0 (See supporting information, Figure S6). However, RRDE data show a less than four electron process. It is, therefore, concluded that in alkaline media, the ORR reaction proceeds via two consecutive two-electron reduction processes, with the formation of peroxide as an intermediate (Figure S7, supporting information). The peroxide however is very unstable and immediately converts into water by the second two-electron step, which has a very high rate constant (See *Introduction*). Therefore, these amido complexes are more efficient ORR electrocatalysts in alkaline media. Further studies need to be conducted to stabilize the complexes in strongly acidic media or alkaline media by suitable structural changes of the ligands around the metal (MN_4) center.

It is proposed that the mechanism of oxygen reduction by these Co(III) amido complexes involves the Co(III) catalytic center responsible for the binding to the oxygen and converting it to water. The ORR process in acid media is represented by Eqs. (1) and (2) and the same in alkaline media by Eqs. (3) and (4) below.

$$\text{Amido} - \text{Co(III)} + O_2 \rightarrow \text{Amido} - \text{Co(IV))} - O - O \quad (1)$$

$$\text{Amido} - \text{Co(IV)} - O - O + 4H^+ + 4e^- \rightarrow \text{Amido} - \text{Co(III)} + 2H_2O \quad (2)$$

$$\text{Amido} - \text{Co(III)} + O_2 + H_2O + 2e^- \rightarrow \text{Amido} - \text{Co(IV)} - HO_2^- + OH^- \quad (3)$$

$$\text{Amido} - \text{Co(IV)} - HO_2^- + H_2O + 2e^- \rightarrow \text{Amido} - \text{Co(III)} + 3OH^- \quad (4)$$

4. Conclusion

We have synthesized amido cobalt complexes with different pendent groups on the benzene ring system to observe the electron withdrawing group on the aromatic ring driving the reduction potential towards positive side compared to moderate electron withdrawing groups. MWCNTs-supported catalysts showed higher ORR catalytic activity and current density due to π–π stacking interactions with nanotubes. Even though these complexes are unstable in strongly acidic or alkaline media, MWCNTs-supported complexes were much stable at moderate pH conditions at which oxygen reduction reaction could be possible with four electron mechanisms. These electrocatalysts are easily drop-casted and studied for the oxygen reduction reaction in various pH conditions at room temperature. However, the electrocatalyst could be a suitable choice for ORR activity in microbial fuel cells (MFCs) and enzymatic biofuel cells (EBCs), where ORR activity can be utilized in neutral, weakly acidic or weakly basic environments to produce electricity.

Acknowledgements

The authors gratefully acknowledge the financial support of a NASA RID (Research Infrastructure Development) grant EPSCoR, NASA RID 11113 and Department of Chemistry, University of Arkansas at Little Rock.

Appendix A. Supplementary data

Supplementary data associated with this article can be found, in the online version, at http://dx.doi.org/10.1016/j.cplett.2013.02.046.

References

[1] Q.C. Le, M.R. Raupach, J.G. Canadell, G. Marland, L. Bopp, P. Ciais, T.J. Conway, et al., Nat. Geosci. 2 (2009) 831.
[2] J. Brouwer, Curr. Appl. Phys. 10 (2010) S9.
[3] M.Z. Jacobson, W.G. Colella, D.M. Golden, Science 308 (2005) 1901.
[4] M.G. Schultz, T. Diehl, G.P. Brasseur, W. Zittel, Science 302 (2003) 624.
[5] V. Dusatre, Nature 414 (2001) 345.
[6] Report of the DOE Basic Energy Sciences Workshop on Hydrogen Production, Storage, and Use, May 13–15, 2003.
[7] J.M. Bowden, J.M. Norbeck, Hydrogen Fuel for Surface Transportation, Society of Automotive Engineers, Warrendale, PA, 1996.
[8] G. Brumfiel, Nature 422 (2003) 104.
[9] L. Carrette, K.A. Friedrich, U. Stimming, Fuel Cells 1 (2001) 5.
[10] P. Costamagna, S. Srinivasan, J. Power Sources 102 (2001) 253.
[11] Fuel Cell Handbook, EG&G Technical Services Inc, 7th Ed U.S. Department of Energy, Office of Fossil Energy, National Energy Technology Laboratory, 2004.
[12] R. Bashyam, P. Zelenay, Nature 443 (2006) 63.
[13] D.J. Berger, Science 286 (1999) 49.
[14] N. Ramaswamy, S. Mukerjee, Adv. Phys. Chem. 2012 (2012) 17.
[15] R. Othman, A.L. Dicks, Z. Zhu, Int. J. Hydrogen Energy 37 (2012) 357.
[16] H.A. Gasteiger, S.S. Kocha, B. Sompalli, F.T. Wagner, Appl. Catal. B 56 (2005) 9.
[17] B. Wang, J. Power Sources 152 (2005) 1.
[18] R.J. Jasinski, Nature 201 (1964) 1212.
[19] F.C. Anson, C. Shi, B. Steiger, Acc. Chem. Res. 30 (1997) 437.
[20] C.J. Chang, Z.-H. Loh, C. Shi, F.C. Anson, D.G. Nocera, J. Am. Chem. Soc. 126 (2004) 10013.
[21] R.P. Kingsborough, T.M. Swager, Chem. Mater. 12 (2000) 872.
[22] K.M. Kadish, L. Fremond, Z. Ou, J. Shao, C. Shi, F.C. Anson, F. Burdet, C.P. Gros, J.-M. Barbe, R. Guilard, J. Am. Chem. Soc. 127 (2005) 5625.
[23] W. Zhang, A.U. Shaikh, E.Y. Tsui, T.M. Swager, Chem. Mater. 21 (2009) 3234.

[24] J.R. McGuire, D.K. Dogutan, T.S. Teets, J. Suntivich, Y. Shao-Horn, D.G. Nocera, Chem. Sci. 1 (2010) 411.
[25] A. Morozan, S. Campidelli, A. Filoramo, B. Jousselme, S. Palacin, Carbon 49 (2011) 4839.
[26] S. Cheng, B.E. Logan, Proc. Natl. Acad. Sci. USA. 104 (2007) 18871.
[27] I. Willner, G. Arad, E. Katz, Bioelectrochem. Bioenerg. 44 (1998) 209.
[28] T. Chen, S.C. Barton, G. Binyamin, Z. Gao, Y. Zhang, H.-H. Kim, A. Heller, J. Am. Chem. Soc. 123 (2001) 8630.
[29] E.H. Yu, S. Cheng, B.E. Logan, K. Scott, J. Appl. Electrochem. 39 (2009) 705.
[30] A. Ghosh, F. Tiago de Oliveira, T. Yano, T. Nishioka, E.S. Beach, I. Kinoshita, E. Münck, et al., J. Am. Chem. Soc. 127 (2005) 2505.
[31] A. Ghosh, D.A. Mitchell, A. Chanda, A.D. Ryabov, D.L. Popescu, E.C. Upham, G.J. Collins, et al., J. Am. Chem. Soc. 130 (2008) 15116.
[32] A. Ghosh, P. Ramidi, S. Pulla, S. Sullivan, S. Collom, Y. Gartia, P. Munshi, A. Biris, B. Noll, B. Berry, Catal. Lett. 137 (2010) 1.
[33] W. Orellana, Phys. Rev. B 84 (2011) 155405.
[34] J. Qu, Y. Shen, X. Qu, S. Dong, Electroanalysis 16 (2004) 1444.
[35] D. Baskaran, J.W. Mays, X.P. Zhang, M.S. Bratcher, J. Am. Chem. Soc. 127 (2005) 6916.
[36] H. Murakami, T. Nomura, N. Nakashima, Chem. Phys. Lett. 378 (2003) 481.
[37] W.R. Carmody, J. Chem. Educ. 38 (1961) 559.
[38] P. Choi, N.H. Jalani, R. Datta, J. Electrochem. Soc. 152 (2005) A1548.
[39] J.H. Zagal, M.A. Gulppi, G. Cárdenas-Jirón, Polyhedron 19 (2000) 2255.
[40] J.A. Streeky, D.G. Pillsbury, D.H. Busch, Inorg. Chem. 19 (1980) 3148.
[41] X.-R. Li, B. Wang, J.-J. Xu, H.-Y. Chen, Electroanalysis 23 (2011) 2955.